Title	Electric Springs for Reducing Power Imbalance in Three-Phase Power Systems
Author(s)	YAN, S; Tan, SC; Lee, CK; Balarko, C; Hui, SYR
Citation	IEEE Transactions on Power Electronics, 2015, v. 30 n. 7, p. 3601-3609
Issued Date	2015
URL	http://hdl.handle.net/10722/209307
Rights	Creative Commons: Attribution 3.0 Hong Kong License

Electric Springs for Reducing Power Imbalance in Three-Phase Power Systems

Shuo Yan, Siew-Chong Tan, *Senior Member, IEEE*, Chi-Kwan Lee, *Senior Member, IEEE*, Balarko Chaudhuri, *Senior Member, IEEE*, and S. Y. Ron Hui, *Fellow, IEEE*

***Abstract*—Electric springs have been used previously in stabilizing mains voltage fluctuation in power grid fed by intermittent renewable energy sources. This paper describes a new three-phase electric spring circuit and its new operation in reducing power imbalance in the three-phase power system of a building. Based on government energy use data for tall buildings, the electric loads are classified as critical and noncritical loads so that building energy model can be developed. The proposed electric spring is connected in series with the noncritical loads to form a new generation of smart loads. A control scheme for such smart loads to reduce power imbalance within the building's electric power system has been evaluated initially with an experimental prototype and then in a system simulation study. The results have confirmed the effectiveness of the new three-phase electric springs in reducing power imbalance and voltage fluctuation, making the building loads adaptive to internal load changes and external mains voltage changes.**

***Index Terms*—Adaptive systems, electric springs (ESs), power imbalance, smart grids, smart loads.**

I. Introduction

With increasing penetration of intermittent and distributed renewable energy sources such as wind and solar power, there has been rising concern on power system stability. To address those issues, many demand-side management techniques have been proposed to ensure the balance between power generation and consumption. Such techniques include: 1) scheduling of delay-tolerant power demand tasks; 2) use energy storage to compensate peak demand; 3) real-time pricing; 4) direct load control or on–off control of smart load. Energy storage is a valid solution to cope with the instantaneous balance between power supply and demand. However, costs and limited energy storage capacity of batteries are practical issues. Therefore, new solutions that can reduce energy storage are preferred.

Manuscript received May 30, 2014; accepted August 9, 2014. Date of publication August 21, 2014; date of current version February 13, 2015. This work was supported by the Hong Kong Research Council under Grant HKU10/CRG/10 and the UK Engineering & Physical Sciences Research Council under Grant EP/K006274/1. Recommended for publication by Associate Editor J. R. Espinoza.

S. Yan, S.-C. Tan, and C.-K. Lee are with the Department of Electrical and Electronic Engineering, The University of Hong Kong, Pokfulam, Hong Kong (e-mail: yanshuo@connect.hku.hk; sctan@eee.hku.hk; cklee@eee.hku.hk).

B. Chaudhuri is with the Department of Electrical and Electronic Engineering, Imperial College London, London SW7 2AZ, U.K. (e-mail: b.chaudhuri@imperial.ac.uk).

S. Y. R. Hui is with the Department of Electrical and Electronic Engineering, The University of Hong Kong, Pokfulam, Hong Kong, and also with the Imperial College London, London SW7 2AZ, U.K. (e-mail: ronhui@eee.hku.hk).

Color versions of one or more of the figures in this paper are available online at http://ieeexplore.ieee.org.

Digital Object Identifier 10.1109/TPEL.2014.2350001

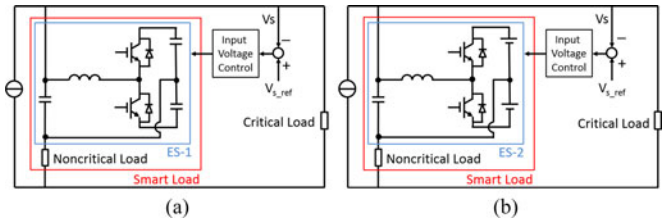

Fig. 1. Practical power circuit implementation of ES. (a) ES version-1. (b) ES version-2.

Electric spring (ES) is a new smart grid technology [1] that can provide electric active suspension functions for voltage and frequency stability in a distributed manner for future smart grid. Based on Hooke's law, ES has been practically realized with power electronic circuits for improving both voltage and frequency stability in microgrid hardware simulator. The same functions for voltage and frequency stability have also been successfully evaluated in a simulation study for a medium-sized power system comprising several power generators. So far, three versions of ES have been conceived. In [1], the fundamental working principles and practical implementation of the first generation of ES (i.e., ES-1) with capacitive storage have been reported. By working under inductive and capacitive mode, ES-1 is capable of regulating the mains voltage to its nominal value in the presence of intermittent power injected into the power grid. With input voltage control, ES can work with noncritical loads that have high tolerance of voltage fluctuation (e.g., with operating voltage range from 180 to 265 V for a nominal mains voltage of 220 V). Examples of the noncritical loads are thermal loads such as ice-thermal storage systems, electric water heater systems, air-conditioning systems, and some public lighting systems.

The first version of ES provides only reactive power compensation for mains voltage regulation and simultaneously varies the noncritical load power so as to achieve automatic power balancing within the power capability of the ES and its associated noncritical load. The study in [2] introduces the second version of ES (i.e., ES-2) by replacing capacitors with batteries on dc link. This arrangement allows ES-2 to work in eight different operating modes and to provide both active and reactive power compensation. It also enables ES-2 to perform extra tasks such as power factor correction and load compensation. The first and second versions of ES are illustrated in Fig. 1(a) and (b), respectively. Note that these two versions of ES are connected in series with their respective noncritical loads. The active suspension concept can also be incorporated into the input control of

grid-connected bidirectional power converters [3] for reducing voltage and frequency instability in the power grid. Such approach can be considered as the third version of ES (i.e., ES-3) that does not need a series noncritical load.

The use of ES for reducing system instability [1], [2] and reducing energy storage requirement [4] in a power grid with substantial penetration of intermittent renewable power has been demonstrated previously. The superior performance of ES over STATCOM in distributed voltage control has just been reported [5]. ES is an emerging technology that deserves more investigations in order to explore its full application potential. This project focuses on its ability for reducing power imbalance in a three-phase system.

Power imbalance is a common and major power quality issue in a three-phase four-wire power system due to the load imbalance in the three phases. Unbalanced line current adversely affects key components in a power system and other equipment such as induction motors, power electronic converters and drives [6]. Severe power imbalance leads to excessive neutral current, increased loss, and reduced power efficiency [7]. Furthermore, the asymmetric voltage drop as a result of imbalanced line current could result in asymmetric voltages in the network, leading to deterioration of overall power quality [8]. Conventional methods to address this issue (such as using a three-phase to two-phase transformer, using rotating equipment to absorb negative sequence component, and using three-phase to single-phase rotary or static converter to feed single-phase load [9]) are of low efficiency and are costly. Modern power electronics technology has offered new solutions to tackle power system quality issues. For example, shunt active filter (AF) in the form of a current-based or voltage-based reactive power compensator has been proposed for reducing load imbalance. So, a mixture of methods can be used, including: 1) using the shunt AF to redistribute real power among three phases when the total amount of active power remains the same; and 2) compensating positive, negative, and zero sequence component separately or jointly. Various techniques of using active power filters for improving power quality and reducing power imbalance can be found in [7], [10]–[14].

In this paper, a new three-phase ES topology is proposed and its operating principle is explained. This new circuit is based on the second version of ES. Besides its ability to enhance the power system stability, its extra use for reducing power imbalance in a three-phase power system in a tall building will be demonstrated in a simulation study, with the support of experimental results obtained from a hardware prototype of the three-phase ES. The paper is an extension of a short conference paper previously presented in [15]. The essence of the incorporation of the ES into noncritical loads is to create a new form of smart or adaptive loads that can help stabilizing the power system as well as reducing power imbalance.

II. Principle of Three-Phase ESs

A. Architecture of a Three-Phase ES in the Power Grid

The three-phase ES is an extension of the single-phase ES recently proposed in [1] and [2]. Fig. 2 shows the circuit diagram

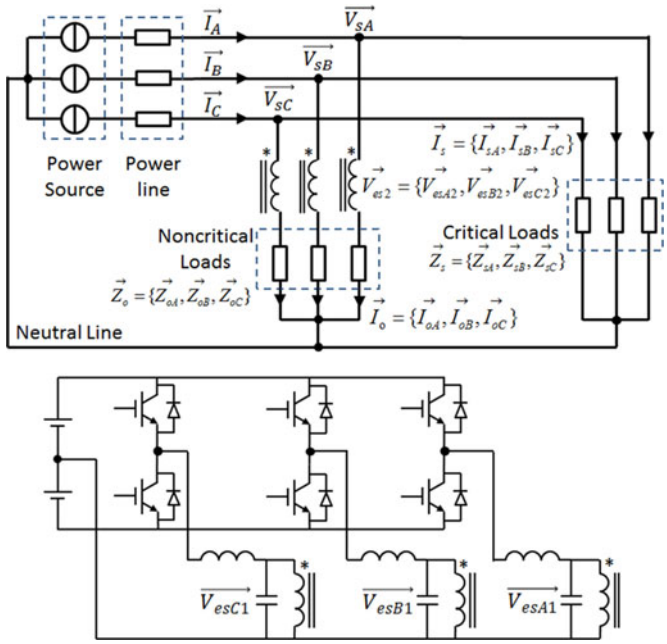

Fig. 2. Circuit diagram and placement of a three-phase ES.

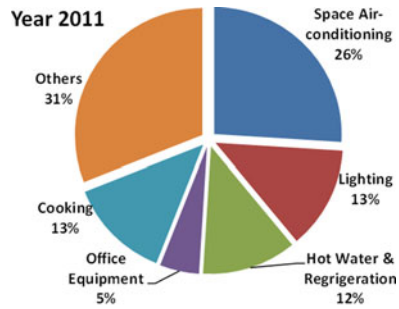

Fig. 3. Typical energy usage in commercial buildings [16].

of a three-phase ES and its placement in a typical three-phase power system. A three-phase ES takes the form of a three-phase inverter with a small battery storage on its dc link and an *LC* filter in the output of each inverter leg. The ac voltage output of each phase is connected to the primary side of an isolation transformer. Through the transformer's turns ratio, the secondary-side voltage is represented as $\vec{V_{\rm es2}} = \{\vec{V_{\rm es}A2}, \vec{V_{\rm es}B2}, \vec{V_{\rm es}C2}\}$. The secondary sides of three isolation transformers are in series connection with three noncritical loads $\vec{Z_o} = \{\vec{Z_{oA}}, \vec{Z_{oB}}, \vec{Z_{oC}}\}$ in star connection with the neutral line connected to the neutral point of three-phase power source. In this example, critical loads $\vec{Z_s} = \{\vec{Z_{sA}}, \vec{Z_{sB}}, \vec{Z_{sC}}\}$ in star connection are connected in parallel with the branches of isolation transformers and noncritical loads. The neutral point of critical load is connected to the neutral point of power source.

Based on published data [16] of the Hong Kong government (see Fig. 3), noncritical loads such as space conditioning, hot water and refrigeration and lighting contribute to about 50% of the total power consumption in commercial buildings. Particularly for tall commercial buildings in Singapore and Hong Kong, the

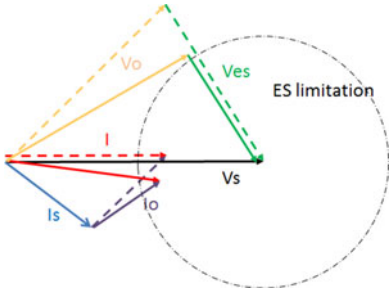

Fig. 4. Compensation vector diagram of ES for current compensation with consideration of physical limitation.

heat pump systems (heating and cooling systems) are dominant electric loads in buildings. Therefore, the three-phase ES can be applied to such loads for providing a series of new features for the power systems within the building infrastructure.

B. Limits of ES

Like mechanical spring which can expand and contract within a certain displacement, ES can only regulate line current within a certain range. Since the three-phase ES is physically a three-phase inverter with a constant dc voltage link, the output voltage of ES is limited by the dc-link voltage $V_{\rm dc}$. In addition, while the noncritical loads may be tolerant to a wide line voltage fluctuation, there still exists a minimum voltage for the noncritical loads in order that these loads can still function within the specifications. For example, some lighting systems have an operating input phase voltage in the range of 80–120 V for the market with a nominal mains voltage of 110 V, and 170–265 V for the markets using 230 V as nominal mains voltage. If the noncritical load is a heating system, the minimum load voltage can be theoretically zero. This means that compensation voltage vector $\vec{V_{\rm es}}$ can vary in amplitude subject to the limitation of the dc-link voltage $V_{\rm dc}$ and have a phase angle for 0–360° with respect to the reference vector which is usually mains voltage of phase A in a three-phase power system. This concept can be more readily understood, if $\vec{Z_o}$(noncritical load) is considered as symmetric pure resistive and $\vec{Z_s}$(critical load) as symmetric resistive plus inductive load. The compensation vector diagram based on this scenario is given in Fig. 4, where the red dash vector is the expected line current. To achieve this optimal compensation, the voltage vector $\vec{V_{\rm es}}$ (green dash vector) shows the voltage that needs to be generated by the ES. When the mains voltage $\vec{V_s}$ remains constant, the sum of the noncritical load current $\vec{I_o}$ (purple dash vector) and critical load current $\vec{I_s}$ (blue solid vector) form the line current.

If the limitation of the ES is considered (highlighted in Fig. 4 as the black dash circle), the ES voltage $\vec{V_{\rm es}}$ must be replaced by the green solid vector. The consequential noncritical load current $\vec{I_o}$ and line current $\vec{I}$ are given by respectively purple solid vector and red solid vector. It is easy to observe that the final line current $\vec{I}$ (red solid vector) deviates from the optimal compensation given in red dash vector both in phase and amplitude. Based on the analysis, the limitation of ES is significant in designing a practical ES control system and in understanding the performance of ES.

III. Three-Phase ES for the Reduction of Line Current Imbalance

In this study, it is assumed that the critical loads are unbalanced among the three phases and the noncritical loads are balanced loads (e.g., a large thermal load such as electric heater system). The sum of power consumptions in the noncritical loads and critical loads represents the total power consumption of a tall building. The loss of balance in a three-phase power grid can be mathematically expressed by (1) when the compensation voltage generated by three-phase ES is treated as $0\angle 0°$ V. Without compensation, the line currents are unbalanced due to the asymmetric load impedance of the critical loads and are given by

$$\begin{cases} \vec{I_A} = \left(\dfrac{1}{\vec{Z_{sA}}} + \dfrac{1}{\vec{Z_{oA}}}\right)\vec{V_{sA}} - \dfrac{1}{\vec{Z_{oA}}}\vec{V_{\rm esA}} \\ \vec{I_B} = \left(\dfrac{1}{\vec{Z_{sB}}} + \dfrac{1}{\vec{Z_{oB}}}\right)\vec{V_{sB}} - \dfrac{1}{\vec{Z_{oB}}}\vec{V_{\rm esB}} \\ \vec{I_C} = \left(\dfrac{1}{\vec{Z_{sC}}} + \dfrac{1}{\vec{Z_{oC}}}\right)\vec{V_{sC}} - \dfrac{1}{\vec{Z_{oC}}}\vec{V_{\rm esC}}. \end{cases} \tag{1}$$

The three-phase ES can be used to reduce the imbalance of a power system. From (1), it can be seen that the three-phase ES voltage $\vec{V_{\rm es}} = \{\vec{V_{\rm esA}}, \vec{V_{\rm esB}}, \vec{V_{\rm esC}}\}$ can be controlled to actively alter the line currents both in amplitude and phase within its operating limits, in response to the changing states of the critical loads. The reduction of power imbalance can be illustrated by the reduction of neutral current, as a large current results in unnecessary conduction losses in the cables of the building's power system. Thus, the equation of the neutral current (2) is a convenient and direct indication for the current imbalance

$$\begin{aligned} \vec{I_{\rm neutral}} = & \left(\frac{1}{\vec{Z_{sA}}} + \frac{1}{\vec{Z_{oA}}}\right)\vec{V_{sA}} - \frac{1}{\vec{Z_{oA}}}\vec{V_{\rm esA}} \\ & + \left(\frac{1}{\vec{Z_{sB}}} + \frac{1}{\vec{Z_{oB}}}\right)\vec{V_{sB}} - \frac{1}{\vec{Z_{oB}}}\vec{V_{\rm esB}} \\ & + \left(\frac{1}{\vec{Z_{sC}}} + \frac{1}{\vec{Z_{oC}}}\right)\vec{V_{sC}} - \frac{1}{\vec{Z_{oC}}}\vec{V_{\rm esC}}. \end{aligned} \tag{2}$$

Furthermore, the reduction of neutral current actually means more in reduction in amplitude of neutral current than in phase angle, so the reduction of line current imbalance can be more precisely expressed by the minimization of neutral current amplitude given by (2), in which the variable-set ($|\vec{V_{\rm esA}}|$, $\theta_{V\,{\rm esA}}$, $|\vec{V_{\rm esB}}|$, $\theta_{V\,{\rm esB}}$, $|\vec{V_{\rm esC}}|$, $\theta_{V\,{\rm esC}}$) is subjected to the limitations of the ES, which is mathematically expressed as

$$\begin{cases} 0 \le |\vec{V_{\rm esA}}|, |\vec{V_{\rm esB}}|, |\vec{V_{\rm esC}}| \le V_{\rm dc} \\ 0° \le \theta_{V\,{\rm esA}}, \theta_{V\,{\rm esB}}, \theta_{V\,{\rm esC}} \le 360°. \end{cases} \tag{3}$$

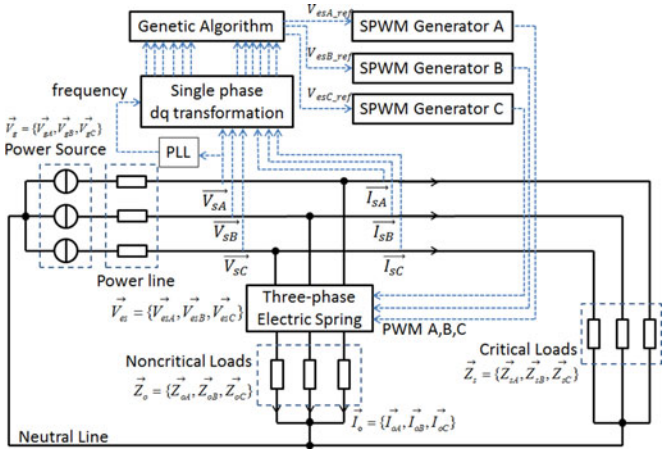

Fig. 5. Block diagram of the implementation and control of a three-phase ES.

IV. Implementation and Control of Three-Phase ES for the Reduction of Line Current

The proposed three-phase ES has been evaluated in both experimental and simulation studies. Fig. 5 shows the schematic of the control system. The three-phase ES is simplified and expressed as three-phase compensation voltage: $\vec{V_{\rm es}} = \{\vec{V_{{\rm es}A}}, \vec{V_{{\rm es}B}}, \vec{V_{{\rm es}C}}\}$.

The power inverter needs to operate in a special manner based on a few arrangements uniquely designed for three-phase ES for line current balance. Besides the power inverter, a feasible three-phase ES system includes a data acquisition and processing block which accepts instantaneous information of the line currents and voltages, and performs *d–q* transformation. A genetic algorithm (GA)-based controller that computes the optimized reference for the three-phase ES, three independent sinusoidal pulse-width-modulated (SPWM) generators, and a phase-locked loop (PLL) block that synchronizes all acquired data within one *d--q* frame rotating at fundamental frequency of 50 Hz are also needed. The power inverter legs are operated independently as half-bridge inverters by receiving PWM signals from their respective SPWM generators.

A. PLL

To acquire accurate feedback, all variables in a three-phase ES system should be synchronized under a fixed fundamental frequency. This is realized by the installation of a PLL block which generates the fundamental system frequency and provides a reference vector with 0° phase angle. As shown in Fig. 5, the PLL block receives the instantaneous information of the mains voltage $\vec{V_{sA}}$ and locks its phase to zero degree. The mains voltage $\vec{V_{sA}}$ is therefore used as the reference vector for other vector variables. Based on this setup, the mains voltages of phases A, B, and C are, respectively, 0°, 240°, and 120°.

B. Single-Phase d–q Transformation

Three-phase *d–q* transformation has been used for the study of a balanced three-phase system. However, this method is based on the assumption that the summation of instantaneous three-phase line currents and voltages equals to zero. This condition makes the classic *d–q* transformation no longer suitable for an unbalanced three-phase system.

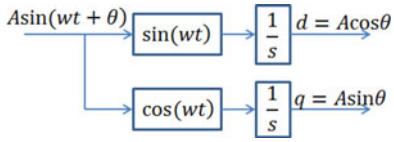

Fig. 6. Single-phase *d–q* transformation.

Fig. 6 shows single-phase *d–q* transformation that decouples each current and voltage independently into d and q components. With the implementation of a PLL block, the decoupled voltages and currents are combined together into one *d–q* frame rotating at fundamental frequency of 50 Hz. The instantaneous currents and voltages are multiplied by sinusoidal and cosinusoidal functions with a fundamental frequency provided by the PLL. The instantaneous products are fed to integrators to filter out the ac components. The d and q components are mathematically described as follows:

$$d = A\cos\theta = \frac{2}{T}\int_{T_n}^{T_{n+1}} A\sin(wt+\theta)\sin(wt)dt \tag{4}$$

$$q = A\sin\theta = \frac{2}{T}\int_{T_n}^{T_{n+1}} A\sin(wt+\theta)\cos(wt)dt. \tag{5}$$

where the symbol A refers to the amplitude of currents or voltages, w is the fundamental angular frequency at which all decoupled d and q components are rotating, and θ is the angle of currents or voltages with respect to the reference vector whose phase angle is tracked to zero degree by the PLL.

C. GA-Based Controller

GA is a popular optimization method for locating the global maximum or minimum values of an objective function within the given range. The optimization process is described in Fig. 7. In a practical implementation, the objective function is to minimize the neutral current. Equation (2) shows that there are six variables whose values are to be optimized in order to achieve the objective. Fig. 7 shows the flowchart of the GA implementation. The GA starts with a group of 100 randomly selected solutions within the limitation given by (3). This group of solutions gives the fitness values of the first generation. In this implementation, the fitness value of GA is equal to the value of the objective function (2). The latter generation is formed after the first generation goes through genetic evolution including mutation, crossover, and migration. When the evolution process is finished, the fitness values of a new generation will be computed. The best fitness value and its corresponding solution will be recorded for further use. The algorithm will continue until the objective function is satisfied. In this implementation, the criterion is the tolerance ($e = 10 \times 10^{-5}$) of objective function, which is the difference of the best fitness values (the minimum value of objective function) between the present and the previous

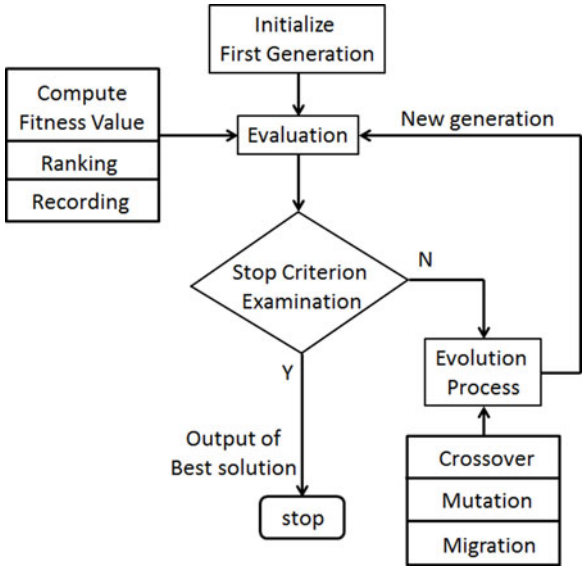

Fig. 7. Flowchart of GA of three-phase ES.

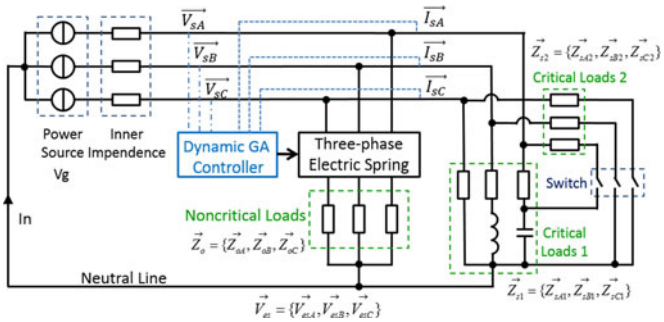

Fig. 8. Experimental setup for testing the hardware prototype of the three-phase ES.

generation. When their difference is smaller than $e = 10 \times 10^{-5}$, the program will stop and the best fitness value and its corresponding solution will be retained and used.

V. Experimental and Simulation Results

In order to evaluate the performance of three-phase ES and the validity of proposed control methodology, a hardware prototype is first evaluated for a laboratory-based three-phase power system. Its characteristics are then modeled and incorporated into an electric energy model of a building (such as a hotel) for large-scale simulation study.

A. Experimental Verification

An experimental setup (see Fig. 8) has been used to test the power balancing function of the new three-phase ES. A three-phase power system supplies power to a set of three-phase noncritical loads and two sets of critical loads. Noncritical loads are loads that can tolerate mains voltage fluctuation larger than the standard tolerance (typically $\pm 5\%$). Examples of such noncritical loads in large buildings are the large-scale water heaters and

TABLE I
Parameters of the Experimental Setup

	Phase A	Phase B	Phase C
$\vec{V_g}$	$200\angle 0°$	$200\angle 240°$	$200\angle 120°$
$\vec{Z_{s1}}(\Omega)$	500 resistive	$250 + 115j$ resistive-inductive	$115 - 115j$ resistive-capacitive
$\vec{Z_{s2}}(\Omega)$	345 resistive	230 resistive	115 resistive
$\vec{Z_{s2}} // \vec{Z_{s1}}(\Omega)$	204 resistive	$119 + 21j$ resistive-inductive	$57.5 - 115j$ resistive-capacitive
$\vec{Z_o}(\Omega)$	200 resistive	200 resistive	200 resistive

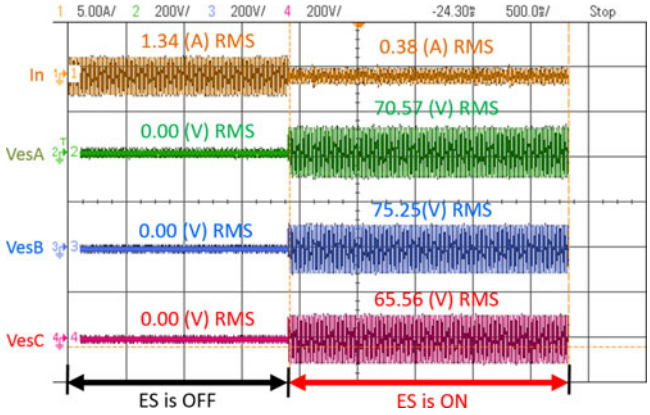

Fig. 9. Measured waveforms of the neutral current of the power system and phase voltage of the three-phase ES.

large-scale cooling systems. These kinds of noncritical loads are assumed to be resistive and balanced in this study. Two sets of critical loads are used because one set will be used to evaluate the performance of the ES for the sudden load change. The parameters for the setup are tabulated in Table I.

Practical tests have been conducted to check the performance of the ES in reducing the power imbalance. The first test is conducted with the noncritical loads and only one set of the critical loads (Z_{s1}). Fig. 9 shows the recorded waveforms of the neutral current and the three-phase voltages of the ES before and after the ES is activated. It can be observed that, without the use of the ES, the neutral current is about 1.34 A. After the ES is activated, the neutral current is reduced by 72% to 0.38 A. It is noted that the three ES voltages are different, meaning that the phase load power consumptions of the balanced three-phase noncritical loads are not identical. Fig. 10(a) and (b) shows the three line currents of the noncritical loads before and after activating the ES, respectively. It can be seen that the three-phase ES is redistributing the line currents of the noncritical loads in order to reduce the power imbalance. For a noncritical load such as a large three-phase electric water heating system, the redistributed heating power within the system will be used to heat up the same tank of water.

In the second test, two different load conditions are used. Initially, only the first set of critical loads is used. Then, both sets of the critical loads are included. The ES is switched off in the interval so that the neutral currents under the two load conditions without activating the ES can be observed. Fig. 11(a)

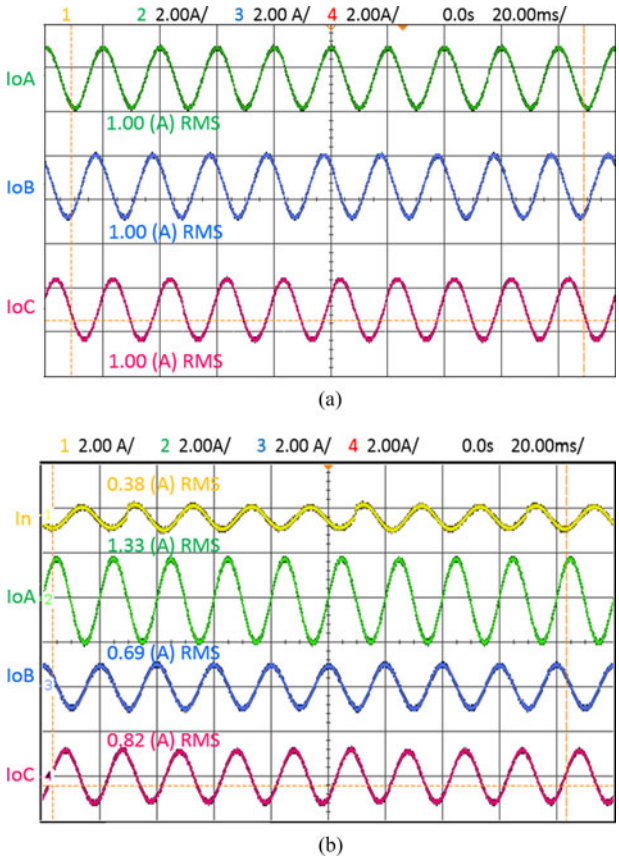

Fig. 10. Measured line currents of the three-phase noncritical loads and the neutral current (a) before and (b) after activating the three-phase ES.

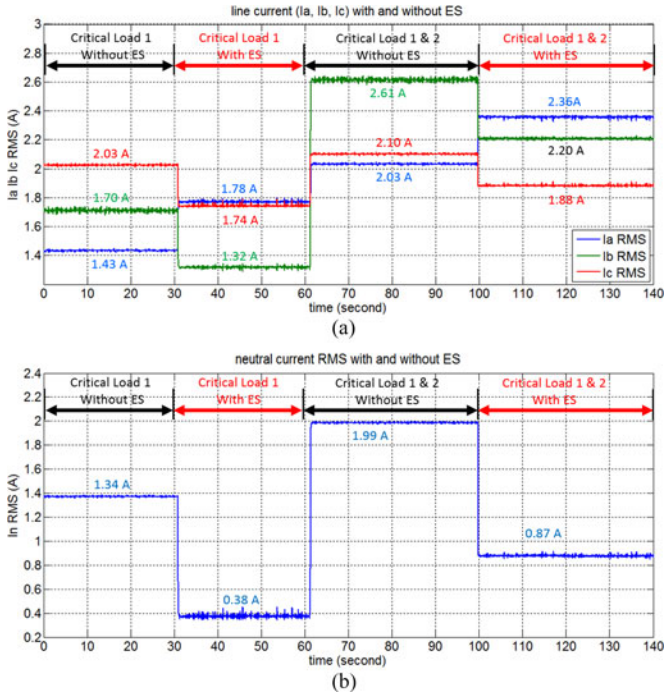

Fig. 11. (a) Measured line currents and (b) measured neutral current of the three-phase system.

TABLE II
SPECIFICATIONS OF ELECTRIC MODEL OF A LARGE HOTEL

	Phase A	Phase B	Phase C
$\vec{Z}_s\,(\Omega)$	$0.075 + 0.425j$ (resistive plus inductive)	$0.157 + 0.298j$ (resistive plus inductive)	$0.171 + 0.171j$ (resistive plus inductive)
$\vec{Z}_o\,(\Omega)$	0.275 (resistive)	0.275 (resistive)	0.275 (resistive)
PF	0.85	0.87	0.90
Computation result of GA			
Best objective function value (theoretical minimized RMS value of neutral current): 1.69×10^{-4} (A)			
No. of generation with the best objective value: 61			
Best solution (optimal three-phase ES voltage): Mag(V)$\angle\theta$ (°)			
$V_{esA} = -43 + 56j = 71(\mathrm{V})\angle 128°$;			
$V_{esB} = -16 + 23j = 28(\mathrm{V})\angle 125°$;			
$V_{esC} = -69 + 77j = 103(\mathrm{V})\angle 132°$.			

shows the three line currents of the three-phase power supply. The corresponding neutral current is shown in Fig. 11(b). It can be seen from Fig. 11(a) that the line currents have been redistributed by the ES and from Fig. 11(b) that the neutral current can be reduced in both cases. In the first load case, the neutral current reduction has been illustrated in Fig. 9. In the second load case, the neutral current is reduced from 1.99 to 0.87 A. These experimental results therefore confirm that the new three-phase ES can be used to reduce power imbalance in a three-phase power system.

B. Building Energy Model and Simulation Study

The building model built in this paper is based on recent publications on energy consumption research of large hotels. According to [17], in 2003, a large hotel in U.S.A. consumes 316 kW·h electric energy per meter square. Perez-Lombard *et al.* [18] point out that up to 68% of consumed energy is used for heating and lighting which can be considered as resistive loads (as lighting systems have power factor correction). Information reported in [17] shows that a typical large hotel has a total area of 122 116 ft^2, which is equal to 11 345 m^2. From the report released by ECS [19], the average power factor of a hotel usually remains between 0.80 and 0.92.

The electric model of a typical hotel is suitable for the implementation of a three-phase ES. Since lighting and heating systems can be considered as resistive loads and are high tolerant to voltage and power fluctuation, they can be used as noncritical loads and be connected in series with the three-phase ES to form the smart loads. Specifications of the equivalent electric model of the three-phase critical and noncritical loads for the hotel building model are given in Table II.

1) Reduction of Current Imbalance: Fig. 12 shows the neutral current of the three-phase power system before and after activating the three-phase ES. The building model shows that the unbalanced loads causes a neutral current of 455 A. After activating the ES, the neutral current has been reduced from 455 A (rms) to 66 A (rms). The three line currents before and after activating the ES are shown in Fig. 13. Again, the current imbalance has been reduced. These results confirm the ability

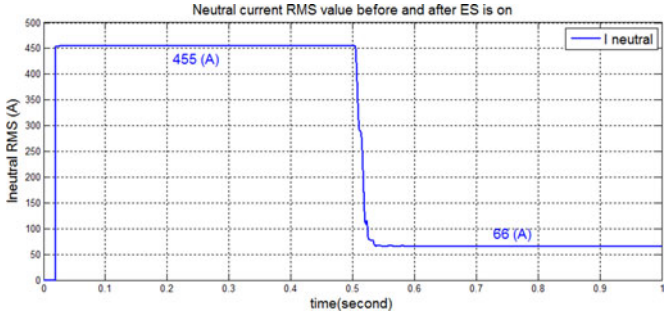

Fig. 12. RMS value of neural current before and after ES is turned on (at $t = 0.5$ s, ES is turned on).

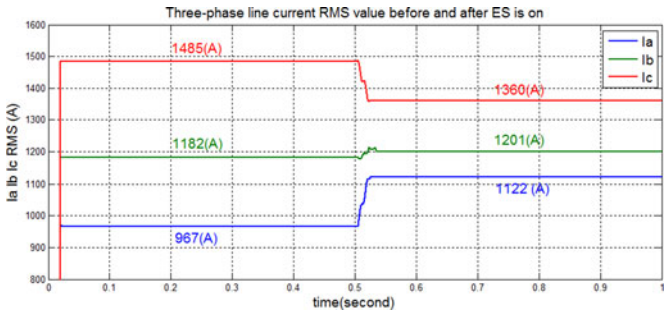

Fig. 13. RMS value of three-phase line current before and after ES is turned on (at $t = 0.5$ s, ES is turned on).

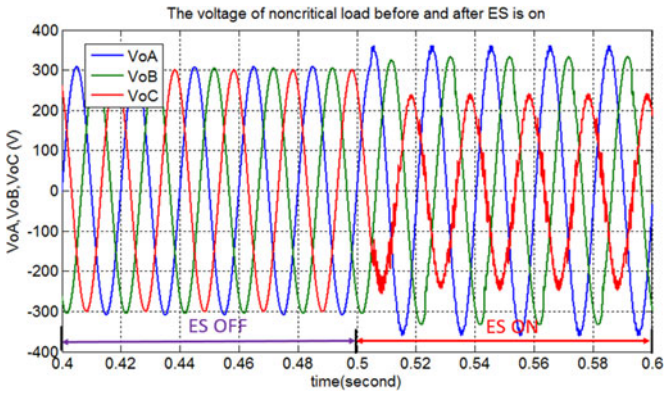

Fig. 14. Steady-state of noncritical load voltage before and after ES is turned on (at $t = 0.5$ s, ES is turned on).

of the ES in reducing power imbalance in a three-phase power system.

The RMS values of three-phase line currents in Fig. 13 show that the current imbalance is reduced. According to the analysis in Section III, the introduction of compensation voltage $\vec{V_{\rm es}} = \{\vec{V_{{\rm es}A}}, \vec{V_{{\rm es}B}}, \vec{V_{{\rm es}C}}\}$ can actively change the power consumption of the noncritical loads. The line currents are altered in the process without affecting the power consumption of the critical loads. Fig. 14 shows the phase voltages of the noncritical loads. It can be seen that the voltage amplitudes are not identical, implying that the noncritical load power consumptions among the three phases are nonidentical. In other words, the reduction of the current imbalance of the three-phase system is made

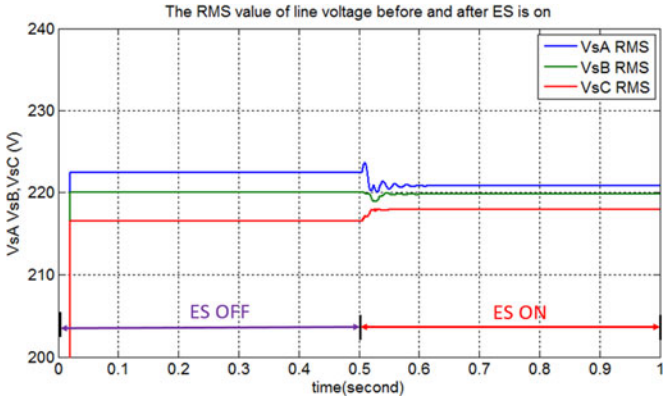

Fig. 15. RMS value of the mains voltage before and after ES is turned on (at $t = 0.5$ s, ES is turned on).

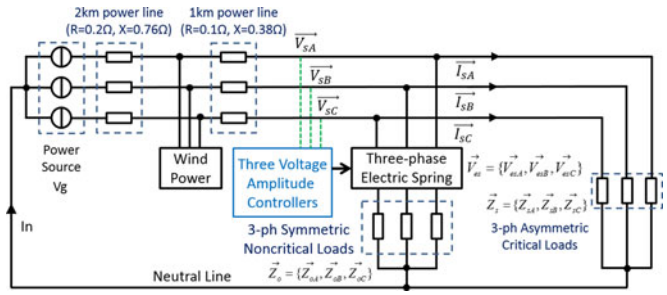

Fig. 16. Simulation setup of a power system with an interrmittent renewable energy source.

possible by the ES in transferring the part of the power imbalance to the noncritical loads.

The constant power supply for the critical loads can be equivalently manifested by the mantainence of line voltage before and after activating the three-phase ES, as shown in Fig. 15. Although the ES does not change the profile of line voltage, the slight variation of mains voltage in RMS value can still be witnessed due to the existence of line impedance and the source impedance of the generator. An interesting by-product worth-mentioning is that the restoration of power balance, equivalently shown by the balance of line current, can help to improve the mains voltage balance. Results in Fig. 15 show that after the ES is turned on, the phase voltage differences among the three phases are reduced.

2) Voltage Stability Improvement: The single-phase ES reported in [1] and [2] provides the stability enhancement for power systems even in the presence of intermittent renewable energy sources such as wind and solar power generators. The proposed three-phase ES retains this useful function. Fig. 16 shows another simulation setup that involves a power network with a traditional generator and a wind power generator. The nominal line-to-neutral voltage of the setup at users' end of the distribution line is 220 V at 50 Hz. A distribution line of 2 km has a resistance of 0.2 Ω and a reactance of 0.76 Ω. Another distribution line of 1 km has a resistance of 0.1 Ω and a reactance of 0.38 Ω. The dc-link voltage of the ES is 240 V. The critical and noncritical loads are listed in Table III.

TABLE III
PARAMETERS OF THE CRITICAL AND NONCRITICAL LOADS

	Phase A	Phase B	Phase C
$\vec{Z}_s\,(\Omega)$ Critical	50 (resistive)	$25 + 11.3j$ (resistive-inductive)	$11.5 - 12.7j$ (resistive- capacitive)
$\vec{Z}_o\,(\Omega)$ Noncritical	2 (resistive)	2 (resistive)	2 (resistive)

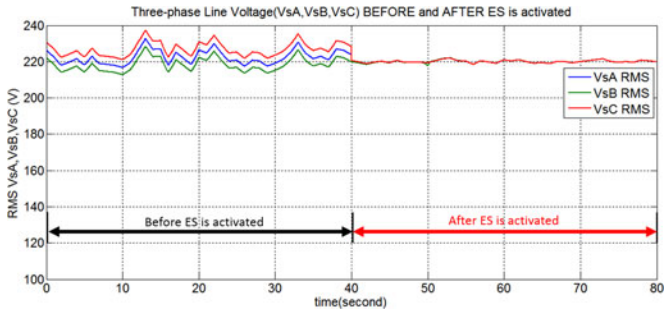

Fig. 17. Simulated mains voltage waveforms of the three-phase power system before and after activating the ES.

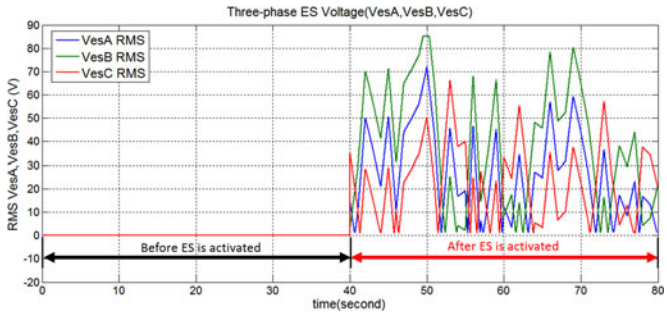

Fig. 18. Simulated ES voltage waveforms of the three-phase power system before and after activating the ES.

The intermittent wind power is simulated by injecting fluctuating current into the power line. Fig. 17 shows the line-to-neutral voltages of the three-phase systems before and after activating the ES. It can be seen that fluctuating power injection into the power line can cause mains voltage fluctuation and the three-phase ES can stabilize the voltage fluctuation as the single-phase counterparts in [1] and [2]. The ES voltage waveforms are shown in Fig. 18. The control of the ES voltages allows the noncritical load power to vary in response to fluctuating wind power generation. Consequently, the mains voltage of the three-phase system can be stabilized even in the presence of an intermittent power source.

VI. CONCLUSION

A new three-phase ES circuit is introduced into the three-phase power system of a building's electric power infrastructure for reducing power imbalance. This is the first study of its kind for smart or adaptive building energy usage. The use of ESs and noncritical loads can form a new generation of smart load that is adaptive to future power supply with intermittent renewable energy sources. The ability of reducing power imbalance in the three-phase system using the three-phase ES has been experimentally verified. Its use with noncritical loads in a building has been successfully evaluated in a simulation study with the building's electric load treated as an adaptive load. The experimental and simulation results show that the ES is effective in reducing power imbalance through redistributing the power in the three-phase noncritical loads. In addition, it retains the power grid voltage regulating function of its single-phase counterpart. With the incorporation of ESs, the equivalent electric loads of buildings can form a new generation of adaptive electric loads that could interact constructively with the dynamically changing nature of future power grid.

REFERENCES

[1] S. Y. R. Hui, C. K. Lee, and F. F. Wu, "Electric springs—A new smart grid technology," *IEEE Trans. Smart Grid*, vol. 3, no. 3, pp. 1552–1561, Sep. 2012.
[2] S. C. Tan, C. K. Lee, and S. Y. R. Hui, "General steady-state analysis and control principle of electric springs with active and reactive power compensations," *IEEE Trans. Power Electron.*, vol. 28, no. 8, pp. 3958–3969, Aug. 2013.
[3] C. K. Lee and S. Y. R. Hui, "Input voltage control bidirectional power converters," US patent application, US2013/0322139, May 31, 2013.
[4] C. K. Lee and S. Y. R. Hui, "Reduction of energy storage requirements for smart grid using electric springs," *IEEE Trans. Smart Grid*, vol. 4, no. 3, pp. 1282–1288, Sep. 2013.
[5] X. Luo, Z. Akhtar, C. K. Lee, B. Chaudhuri, S. C. Tan, and S. Y. R. Hui, "Distributed voltage control with electric springs: Comparison with STATCOM," *IEEE Trans. Smart Grid* early access
[6] A. von Jouanne and B. Banerjee, "Assessment of voltage unbalance," *IEEE Trans. Power Del.*, vol. 16, no. 4, pp. 782–790, Oct. 2001.
[7] S. George and V. Agarwal, "A DSP based optimal algorithm for shunt active filter under nonsinusoidal supply and unbalanced load conditions, and smart loads," *IEEE Trans. Power Electron.*, vol. 22, no. 2, pp. 593–601, Mar. 2007.
[8] B. Singh, K. Al-Haddad, and A. Chandra, "A review of active filters for power quality improvement," *IEEE Trans. Ind. Electron.*, vol. 46, no. 5, pp. 960–971, Oct. 1999.
[9] V. B. Bhavaraju and P. N. Enjeti, "Analysis and design of an active power filter for balancing unbalanced loads," *IEEE Trans. Power Electron.*, vol. 8, no. 4, pp. 640–647, Oct. 1993.
[10] J. W. Dixon, J. J. Garcia, and L. Moran, "Control system for three-phase active power filter which simultaneously compensates power factor and unbalanced loads," *IEEE Trans. Ind. Electron.*, vol. 42, no. 6, pp. 636–641, Dec. 1995.
[11] A. Chandra, B. Singh, B. N. Singh, and K. Al-Haddad, "An improved control algorithm of shunt active filter for voltage regulation, harmonic elimination, power-factor correction, and balancing of nonlinear loads," *IEEE Trans. Power Electron.*, vol. 15, no. 3, pp. 495–506, May 2000.
[12] C.-C. Chen and Y.-Y. Hsu, "A novel approach to the design of a shunt active filter for an unbalanced three-phase four-wire system under nonsinusoidal conditions," *IEEE Trans. Power Del.*, vol. 15, no. 4, pp. 1258–1264, Oct. 2000.
[13] P. Verdelho and G. D. Marques, "An active power filter and unbalanced current compensator," *IEEE Trans. Ind. Electron.*, vol. 44, no. 3, pp. 321–328, Jun. 1997.
[14] W. C. Lee, T. K. Lee, and D. S. Hyun, "A three-phase parallel active power filter operation with PCC voltage compensation with consideration for an unbalanced load," *IEEE Trans. Power Electron.*, vol. 17, no. 5, pp. 807–814, Sep. 2002.
[15] S. Yan, S. C. Tan, C. K. Lee, and S. Y. R. Hui, "Reducing three-phase power imbalance with electric springs," presented at the 5th International Symposium on Power Electronics for Distributed Generation Systems, Galway, Ireland, Jun. 22–25, 2014.
[16] *Hong Kong Energy End-Use Data 2013*, Electrical & Mechanical Services Department, Hong Kong Special Administration Region, 2013.

[17] "M. Deru *et al.*, U.S. Department of Energy Commercial Reference Building Models of the National Building Stock," National Renewable Energy Laboratory, Golden, CO, USA, Tech. Rep. NREL TP-5500-46861, Feb. 2011.
[18] L. Perez-Lombard, J. Ortiz, and C. Pout, "A review on buildings energy consumption information," *Energy Buildings*, vol. 40, pp. 394–398, Mar. 2007.
[19] (2014). [Online]. Available: http://www.ecsintl.com/solutions/power-factor-correction

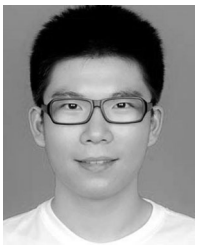

Shuo Yan was born in China, in 1986. He received the Bachelor's degree from the University of South China, Hengyang, China, in 2007, and the master's degree from Southeast University, Nanjing, China, 2010, both in electrical engineering. He is currently working toward the Doctor of Philosophy degree in electrical engineering in the Department of Electrical and Electronic Engineering, The University of Hong Kong, Pokfulam, Hong Kong.

His current research interests include power electronic technology in smart grid, advance control of renewable energy sources, and microgrid.

Siew-Chong Tan (S'00–M'06–SM'11) received the B.Eng. (Hons.) and M.Eng. degrees in electrical and computer engineering from the National University of Singapore, Singapore, Singapore, in 2000 and 2002, respectively, and the Ph.D. degree in electronic and information engineering from the Hong Kong Polytechnic University, Hung Hom, Hong Kong, in 2005.

From October 2005 to May 2012, he was a Research Associate, Lecturer, and Assistant Professor in the Department of Electronic and Information Engineering, Hong Kong Polytechnic University. From January to October 2011, he was Senior Scientist in Agency for Science, Technology and Research (A*Star), Singapore. He is currently an Associate Professor in the Department of Electrical and Electronic Engineering, The University of Hong Kong. He was a Visiting Scholar at the Grainger Center for Electric Machinery and Electromechanics, University of Illinois at Urbana-Champaign, from September to October 2009, and an Invited Academic Visitor of the Huazhong University of Science and Technology, Wuhan, China, in December 2011. He is a coauthor of the book *Sliding Mode Control of Switching Power Converters: Techniques and Implementation* (Boca Raton, FL, USA: CRC Press, 2011). His research interests include power electronics and control, LED lightings, smart grids, and clean energy technologies.

Dr. Tan serves extensively as a Reviewer for various IEEE/IET transactions and journals on power, electronics, circuits, and control engineering.

Chi-Kwan Lee (M'08–SM'14) received the B.Eng. and Ph.D. degrees in electronic engineering from the City University of Hong Kong, Kowloon, Hong Kong, in 1999 and 2004, respectively.

He was a Postdoctoral Research Fellow in the Power and Energy Research Centre at the National University of Ireland, Galway, from 2004 to 2005. In 2006, he joined the Centre of Power Electronics in City University of Hong Kong as a Research Fellow. From 2008 to 2011 he was a Lecturer of electrical engineering with the Hong Kong Polytechnic University. He was a Visiting Academic with Imperial College London from 2010 to 2013. Since January 2012, he has been an Assistant Professor in the Department of Electrical and Electronic Engineering, The University of Hong Kong, Pokfulam, Hong Kong. His current research interests include applications of power electronics to power systems, advanced inverters for renewable energy and smart grid applications, reactive power control for load management in renewable energy systems, wireless power transfer, energy harvesting, and planar electromagnetics for high-frequency power converters.

Balarko Chaudhuri (M'06–SM'11) received the Ph.D. degree in electrical and electronic engineering from Imperial College London, London, U.K., in 2005.

He is currently a Senior Lecturer in the Control and Power Research Group, Imperial College London. His area of interest is electric power transmission systems, control theory, smart grids and renewable energy.

Dr. Chaudhuri a Member of the IET and CIGRE. He is an Associate Editor of the IEEE SYSTEMS JOURNAL and *Elsevier Control Engineering Practice*.

S. Y. Ron Hui (M'87–SM'94–F'03) received the B.Eng. (Hons.) degree from the University of Birmingham, West Midlands, U.K., in 1984, and the D.I.C. and Ph.D. degrees from Imperial College London, London, U.K., in 1987.

He currently holds the Philip Wong Wilson Wong Chair Professorship at the University of Hong Kong, Pokfulam, Hong Kong. Since 2010, he has been a part-time Chair Professor of power electronics with Imperial College London. He has published more than 300 technical papers, including more than 180 refereed journal publications and book chapters. More than 55 of his patents have been adopted by industry.

Dr. Hui is an Associate Editor of the IEEE TRANSACTIONS ON POWER ELECTRONICS and the IEEE TRANSACTIONS ON INDUSTRIAL ELECTRONICS, and an Editor of the IEEE JOURNAL OF EMERGING AND SELECTED TOPICS IN POWER ELECTRONICS. He has been appointed twice as an IEEE Distinguished Lecturer by the IEEE Power Electronics Society in 2004 and 2006. He received the IEEE Best Paper Award from the IEEE IAS in 2002, and two IEEE Power Electronics Transactions Prize Paper Awards in 2009 and 2010. His inventions on wireless charging platform technology underpin key dimensions of Qi, the world's first wireless power standard, with freedom of positioning and localized charging features for wireless charging of consumer electronics. In November 2010, he received the IEEE Rudolf Chope R&D Award from the IEEE Industrial Electronics Society and the IET Achievement Medal (The Crompton Medal). He is a Fellow of the Australian Academy of Technological Sciences and Engineering and is the recipient of the 2015 IEEE William E. Newell Power Electronics Award.